2010 IEEE International Conference on Robotics and Automation
Anchorage Convention District
May 3-8, 2010, Anchorage, Alaska, USA

Scaling Up Shape Memory Alloy Actuators using a Recruitment Control Architecture

Lael Odhner and Harry Asada

Abstract— **This paper presents new experimental results from a human-size robotic forearm, created to demonstrate the effectiveness of recruitment-based control architectures for large actuators made from shape memory alloys (SMA) and other active materials. The robot arm is actuated antagonistically by two actuators made up of 60 small SMA springs arranged in parallel, which are activated in an on/off fashion using Joule heating. The force and stiffness of each actuator is controlled by recruiting a desired number of springs to contract. The joint position is then controlled using equilibrium point servo control. The results presented in this paper show that the combination of equilibrium point control of the arm joint and recruitment-based control of each actuator's stiffness solve some of the major problems of scalability and response speed often associated with active material actuators.**

I. Introduction

The feedback control performance of small-scale shape memory alloys (SMAs) and other active material actuators has improved significantly in recent years. Closed-loop control of large amplitude, air-cooled SMAs has been reported at up to 1 Hz [1], and similar results have been reported for free-standing conducting polymer (CP) actuators [2]. However, these results are limited to materials having characteristic thicknesses on the order of tens to hundreds of microns, because the materials are activated by the diffusion of heat or chemical species, processes that scale up poorly to larger lengths [3]. In order to achieve short response times while producing large amounts of force, some architecture is needed to decouple the length scale of energy transport from the size of the actuator.

This paper demonstrates that an architecture similar to motor recruitment can be used to improve the performance of shape memory alloy actuators. Novel actuators were constructed, made up of many individual SMA units, as shown in Fig. 1, much like skeletal muscle [4]. Each active unit can be made small enough that diffusion is fast. The amount of force available can be scaled up by adding more units to the actuator. The control of such an actuator is hierarchical: Each small unit is either totally relaxed or totally contracted. A single central controller then coordinates the units so that the number of contracted units is sufficient to produce the desired level of force or displacement [5], [6], [7], [8]. Because the activation of a unit is decoupled from the total force produced, the actuator functions at the speed of a single unit, and is capable of producing 30 mm of displacement at 120 N force.

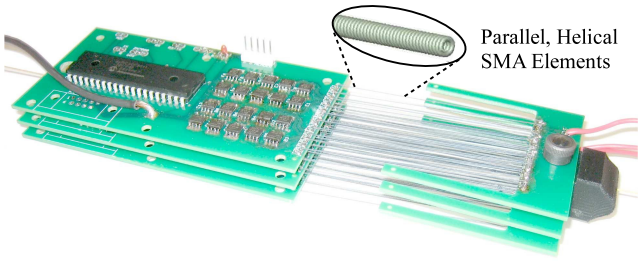

Fig. 1. A photograph of a SMA actuator composed of many small, independent units.

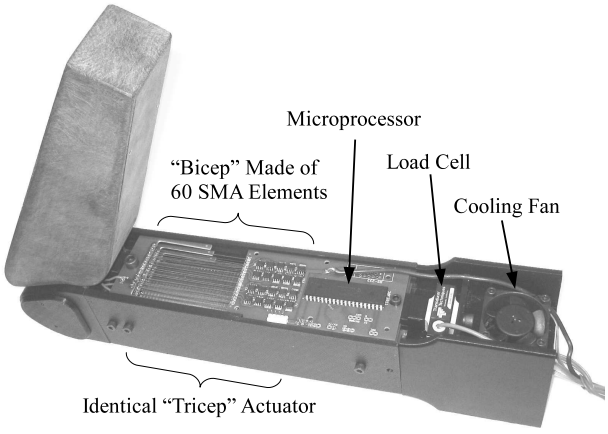

Fig. 2. A photograph of the robot arm.

Two recruitment-based actuators are used in an antagonistic configuration to control a human-sized robot arm, shown in Fig. 2. Due to the physical actuator architecture, these actuators produce a controllable stiffness, rather than a controllable force. The elbow joint angle of this robot arm is controlled using equilibrium point (EP) control, a control system architecture inspired by biological motor control systems [9], [10] that has recently garnered some interest in the robotics community [11]. The use of equilibrium point control has other advantages, because it enables the rejection of high-speed disturbances, despite the relatively slow response of SMA.

The arm design and control system are presented in several sections. Section II introduces the overall design of the robot arm, including the location and configuration of the

This material is based upon work supported by the National Science Foundation under grant number 0143242.

L. Odhner is with the Department of Mechanical Engineering, Yale University, New Haven, CT 06520, USA lael.odhner@yale.edu
H. Asada is with the Department of Mechanical Engineering, Massachusetts Institute of Technology, Cambridge, MA 02139, USA asada@mit.edu

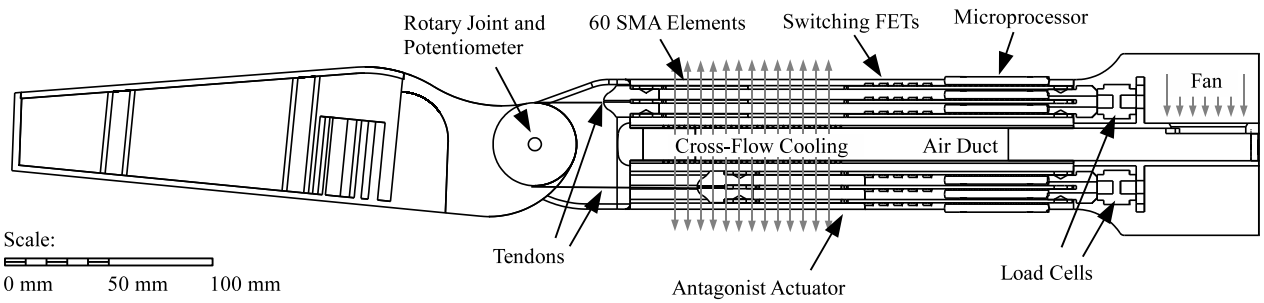

Fig. 3. A section view of the robot arm, showing the integrated cooling system and the force and displacement sensors.

actuators and the sensors for feedback. Section III explains how variable-stiffness antagonistic actuators can be used to control the position of a joint using equilibrium point control. A model of the recruitment-based actuator is derived in Section IV, with a control scheme for modulating the actuator stiffness. Experimental results highlighting the performance benefits of the actuator architecture are presented in Section V.

II. Arm Design

The robot arm used in this work is shown in Fig. 2, and a section view is shown in Fig. 3. The arm was designed to be roughly the size of a human arm; the forearm measures 254 mm from the elbow joint to the stump at the wrist. The elbow joint is actuated by two SMA actuators, arranged as a bicep and tricep on either side of the arm. Each actuator is a 3×20 array of 40 mm long pieces of Toki BioMetal Helix material, a SMA spring that contracts by about 50% of its length when heated [12]. Power is delivered to each SMA element via Joule heating, using transistors that switch 300 mA of current into each wire when the unit is commanded to contract. The contractile state of each element is governed by a small two-state machine, as shown in Fig. 4. The state machines are implemented on microprocessors connected to the driving transistors. The array is constantly cooled using cross-flow forced convection, as depicted in Fig. 3. Air from a fan at the shoulder is blown into an air duct running down the center of the arm. Thin slits in the channel wall let air escape and blow across the SMA wires. Because the heating and cooling of the wires is entirely open-loop, the design of the SMA units was intentionally power limited to avoid burning out any of the SMA wires.

The elbow angle was measured with a potentiometer embedded in the joint. In order to measure the net torque and stiffness of the arm, Transducer Techniques MLP-25 force sensors were placed inline with each actuator, at the shoulder side of the upper arm. These sensors measured only the total force and displacement of the actuator; no information was directly obtained about how many SMA units were recruited at any point in time. A central controller, implemented in LabView on a desktop computer, was used to determine the central commands sent to each SMA unit to move the arm to the desired position.

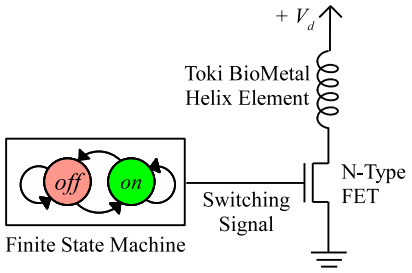

Fig. 4. A schematic of the control circuitry for a single SMA unit.

III. Controlling Joint Position

The elbow joint angle was controlled using equilibrium point (EP) control, a concept that has its roots in the neuroscience community. It has been widely observed that the body appears to use passive muscle stiffness as a stabilizing mechanism for motor control. For example, Bizzi and Polit reported a study in which monkeys were observed performing simple pointing tasks in the presence of disturbance forces after their proprioceptive feedback loops were cut at the spinal column [13]. The best explanation for this phenomenon is that the antagonistic muscles pulling on each joint act as tunable springs in equilibrium when the limb is in its desired posture, as shown in Fig. 5. Thus, even without active feedback, the passive spring force of the muscles serves to stabilize the limb. Many variants on the equilibrium point hypothesis have been proposed; a good summary can be found in [10].

Equilibrium point control has recently received a lot of attention from the robotics community, as a means of designing mechanisms having variable stiffness [14], or as a means of simulating the human body in hardware [15], or as a method of controlling active material actuators [11]. It is specifically of interest to the authors because it is much easier to modulate the stiffness of active material actuators using recruitment than it is to treat the actuators as ideal force or displacement sources. Additionally, EP servo hypotheses have been argued to improve the passive stability of human motor control beyond the performance limitations imposed by the slow rates of neural processing and muscle activation[16]. Some of these very same speed issues are shared by SMA and other active material actuators.

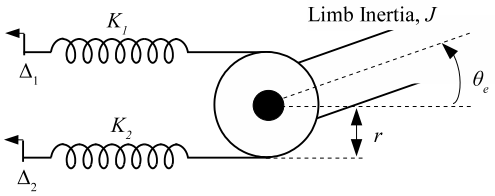

Fig. 5. The mechanics of a joint connected between two antagonistic springs.

Equilibrium point control can mitigate these speed problems in these artificial actuators as well.

A. Equilibrium Point Control

Equilibrium point control can be understood by considering the simplified case of a joint of radius r, having inertia J, connected between two springs, as shown in Fig. 5. Each spring is anchored at a different rest length Δ_1 and Δ_2, and each has a different stiffness K_1 and K_2. The equilibrium position to which the joint is drawn is the average of Δ_1/r and Δ_2/r, weighted by the relative stiffness of each spring,

$$\theta_e = \frac{1}{K_1 + K_2}\left(K_1\frac{\Delta_1}{r} - K_2\frac{\Delta_2}{r}\right) \tag{1}$$

This is analogous to the voltage at the center of a voltage divider. The joint will be stable about θ_e, having a stiffness equal to the sum of the stiffness of the antagonistic springs,

$$K_J = \frac{\partial \tau}{\partial \theta} = r^2(K_1 + K_2) \tag{2}$$

If the joint were perturbed from its equilibrium position and let go, it would return to equilibrium on a time scale related to the resonant frequency of the joint,

$$T_e = \sqrt{J/K_J} \tag{3}$$

This is a purely passive phenomenon unrelated to any active input. If variable stiffness actuators were connected to the joint instead of springs, the dynamics of the passive restoring force would be unaffected by the rate at which the displacements, Δ_1 and Δ_2, or the stiffnesses, K_1 and K_2, can be varied. Thus a slow actuator such as SMA would appear to exert a fast restoring force if equilibrium point control is used.

B. Specifying an Equilibrium Point

Now consider the case when the stiffness of each actuator can be modulated. To move the forearm into a desired position, (1) is used to determine the necessary ratio between the stiffness of the agonist and antagonist actuators:

$$K_1 = -K_2\frac{\theta_e + \Delta_2/r}{\theta_e - \Delta_1/r} \tag{4}$$

Any values of K_1 and K_2 satisfying this constraint will produce the correct equilibrium angle, but more information is needed to fully specify the joint stiffnesses. The authors fully constrained the choice of the desired stiffnesses $K_{1,ref}$ and $K_{2,ref}$ by maximizing the joint stiffness at the desired equilibrium angle. One of the two actuators was always commanded to its maximum stiffness K_{max}. The other was determined by (4) using the measured stiffness of the other actuator,

$$\frac{\theta_e + \Delta_2/r}{\theta_e - \Delta_1/r} > 1: \tag{5}$$

$$K_{1,ref} = K_{max}$$

$$K_{2,ref} = -K_1\frac{\theta_e - \Delta_1/r}{\theta_e + \Delta_2/r}$$

$$\frac{\theta_e + \Delta_2/r}{\theta_e - \Delta_1/r} < 1:$$

$$K_{1,ref} = -K_2\frac{\theta_e + \Delta_2/r}{\theta_e - \Delta_1/r}$$

$$K_{2,ref} = K_{max}$$

Notice that one actuator is always seeking to produce the maximum stiffness while the other sets its stiffness in relation to the first. This ensures that the equilbrium point is reached, even if the actuator cannot quite reach the commanded maximum stiffness.

C. Compensation for Slow Disturbances

One potential pitfall of equilibrium point control is joint compliance. Because the equilibrium trajectory is being controlled, not the actual joint angle, steady state errors due to constant or slowly changing disturbance torques τ_d are inevitable:

$$\theta = \theta_e - \frac{\tau_d}{r^2(K_1 + K_2)} \tag{6}$$

In order to compensate for this, one could estimate the difference between the equilibrium joint position and the perturbed joint position, $\tilde{\theta}$, using a slow, discrete-time averaging filter:

$$\hat{\tilde{\theta}}(t+1) = (1-\rho)\hat{\tilde{\theta}}(t) + \rho(\theta_e - \theta) \tag{7}$$

This value can be added to the desired equilibrium angle θ_e and fed forward into the controller to cancel out the steady state disturbance,

$$\theta_{e,ref}(t) = \theta_e(t) + \hat{\tilde{\theta}}(t) \tag{8}$$

Adaptive cancellation of slow disturbances works as long as the characteristic time scale of the averaging filter is long relative to the characteristic time of the feedback controller. If this is not the case, then there could be possibly problematic interactions between the controller and the estimator.

IV. Controlling Actuator Stiffness

In the previous section, a relationship was derived between the desired equilibrium angle of the joint and the actuator stiffnesses required to produce that equilibrum angle. This section deals with producing this desired actuator stiffness based on the number of recruited actuator units. Some terminology is required to describe the process of recruitment. Consider an actuator made of N units, each having some state $s_i(t) \in \{on, off\}$. The number of units in the on state, $N_{on}(t)$, is a kind of state space description of the recruitment actuator. If the actuator stiffness can be represented in terms

of $N_{on}(t)$, then the problem of producing some desired stiffness can be reduced to the problem of recruiting the desired number of units.

A. Stiffness in Parallel, Recruitment-Based Actuators

Active materials, such as shape memory alloys, are not well represented as ideal force or displacement sources. Instead, it makes more sense to think of each unit of an active material actuator as a spring whose stiffness k_i and rest length δ_i are functions of temperature. The tension force f_i produced by the unit as a function of length d_i is then a piecewise linear function,

$$f_i(d_i) = \begin{cases} k_i(d_i - \delta_i), & d_i > \delta_i \\ 0, & d_i \leq \delta_i \end{cases} \tag{9}$$

The tension must be positive because the SMA springs cannot support a force in compression. When the active material changes state, the parameters k_i and δ_i can change values. The Toki BioMetal Helix elements used for this paper were placed in a mechanical analyzer, and the force-length properties were measured in both the *on* (austenite) and *off* (martensite) states:

$$k_i(s_i) = \begin{cases} 93 \text{ mN/mm}, & s_i = on \\ 83 \text{ mN/mm}, & s_i = off \end{cases} \tag{10}$$

$$\delta_i(s_i) = \begin{cases} 0 \text{ mm}, & s_i = on \\ 20 \text{ mm}, & s_i = off \end{cases} \tag{11}$$

The agreement between the linear model of (9) and the measured force-lengh curves, plotted in Fig.6, is striking. To extrapolate this model to the force-length properties of the whole actuator, consider N active material motor units placed together in parallel. Because the length of each unit is identical, the force F produced by an actuator length D is the sum of each unit's force,

$$F(D) = \sum_i f_i(D) \tag{12}$$

If the actuator displacement is smaller than the *off* displacement, then the *off* units will be slack, and contribute nothing to the actuator force. The total force is then proportional to the number of units in the *on* state,

$$F(D < \delta_{off}) = k_{on} N_{on}(t)(D - \delta_{on}) \tag{13}$$

Thus, the effective stiffness of the actuator $K(t)$ could be written as a linear function of $N_{on}(t)$,

$$K(t) = k_{on} N_{on}(t) \tag{14}$$

Figure 7 shows the force-length curve for the 60 unit experimental actuator, compared to the approximate force-length prediction as computed in (13). The agreement is very good when all of the units are contracted. The stiffness is underpredicted when fewer units are contracted. The most likely explanation for this is that the *off* units are packed next to the *on* units in the actuator array. Some cross-heating of the *off* units occurs, which causes these relaxed units to be partially engaged. It is easy enough to calibrate the model to account for this effect.

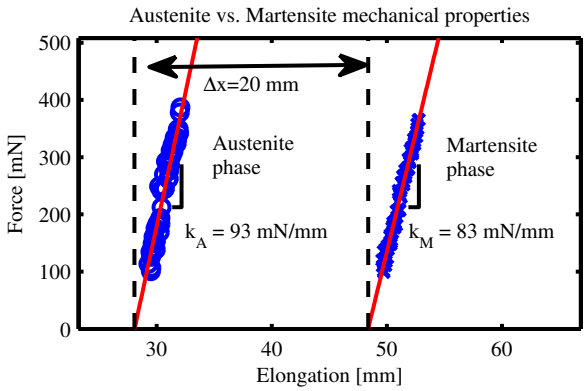

Fig. 6. The force-length relationship of a single SMA element.

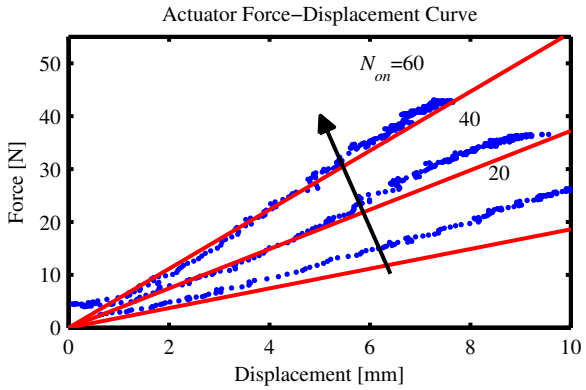

Fig. 7. The measured force-length relationship of the 60 element actuator, compared to the model, based on a single element.

B. Controlling Actuator Stiffness

Equation (13) can be used to predict the force-length relationship as a function of the number of recruited units, $N_{on}(t)$. It can also be used to predict $N_{on}(t)$ based on measurements of an actuator's force and displacement,

$$\hat{N}_{on}(t) = \frac{F(t)}{k_{on}(D - \delta_{on})} \tag{15}$$

A desired stiffness K_{ref} could similarly be translated into a desired number of recruited units, N_{ref} using (14),

$$N_{ref} = \frac{K_{ref}}{k_{on}} \tag{16}$$

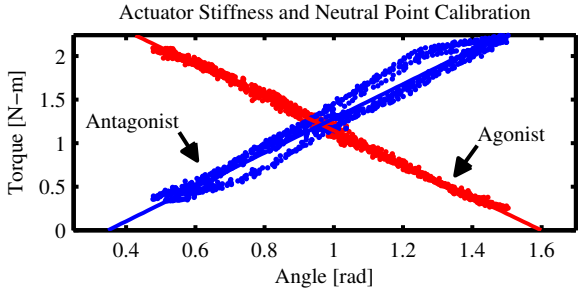

Fig. 8. The *in situ* torque-angle curve of each actuator, with all SMA units active.

Thus, the control problem reduces to one of commanding some number of units to transition from the *off* state to the *on* state, or vice versa. The authors have written several papers on this problem [5], [6]. One robust solution is to design the units so that they make random state transitions whose probabilities are determined by the commands broadcast by the central controller. Thus, a controller broadcasting a command for all units to transition from *off* to *on* with probability 0.5 will get response from approximately half of the un-recruited units. These previous papers contain an in-depth discussion of how to formulate these stochastic recruitment control laws, which will not be repeated here. In the end, the control law used to modulate the stiffness of the actuator was one which set the expected rate of state transitions conditioned on the central controller's commands proportional to the error (the difference between $N_{on}(t)$ and N_{ref}). In order to estimate $N_{on}(t)$, the force sensors and joint angle measurement were calibrated *in situ*, producing a torque-angle plot shown in Fig. 8. This plot shows the force-length curve for both actuators with all of the units recruited, so that K_{max}, Δ_1 and Δ_2 can be identified.

V. Experimental Results

To test the tracking capabilities of the equilibrium point controller, the robot arm was held in the horizontal plane, with the shoulder clamped, as shown in Fig 9. A swept sine reference with a peak-to-peak amplitude of 0.6 radians was fed into the controller. A Bode plot of the gain and phase response of the arm is shown in Fig. 10. The results of the experiment indicate that the 1/2 amplitude bandwidth of the actuator is approximately .146 Hz, corresponding to a period of 7 seconds. Considering that the response time of the underlying shape memory alloy actuators was approximately 5 seconds, this is a good result. If more aggressive methods of controlling shape memory alloys were employed, the underlying material response time, and consequently the closed-loop bandwidth, could be improved. The phase response of the actuator drops linearly off as a function of frequency, suggesting a pure time delay. This time delay was measured and found to be approximately 2 seconds. This, also could be improved by increasing the controller power, and by more carefully regulating the temperature of the SMA wire to ensure that the wire is not becoming too cool in its *off* state or too hot in its *on* state, which could cause a significant time delay while the sensible heat required to bring the SMA to its phase transition temperature is delivered.

A. Joint Angle Tracking

To demonstrate the ability to reject a constant disturbance force using an adaptive estimator, as described in (7), the arm was oriented in the vertical plane, and a square wave reference was commanded. The response, plotted in Fig. 11, shows the joint angle following the desired angle, while the equilibrium point lies offset from the true angle due to the disturbance. The video attached to this paper also demonstrates the arm's ability to adjust to a step load,

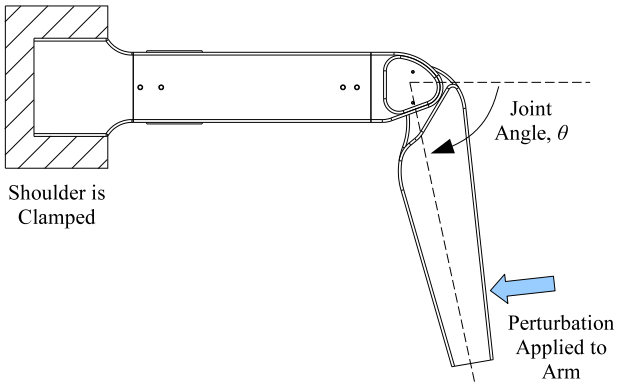

Fig. 9. A diagram of the experiment setup, showing the direction of applied disturbance force.

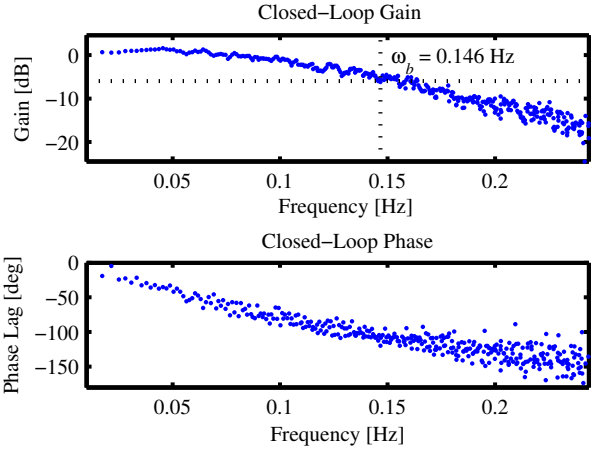

Fig. 10. A Bode plot of the closed-loop actuator response, showing the half amplitude bandwidth.

introduced in the form of a weight placed on the arm (at 0:47). Once the estimator adjusts to the new disturbance force, the arm functions as before, passively rejecting fast disturbances about the desired joint angle.

Some overshoot was observed whenever the arm traveled in one direction. The authors believe that this is caused by the interaction between the controlled stiffnesses of each actuator from (5). Because one actuator is commanded to a reference that is a function of the other actuator's stiffness, the interaction between the two may be causing some unforseen deviation from the desired output. This artifact of two-controller interaction is a subject for future study.

B. Fast Disturbance Rejection

The most fascinating aspect of EP control is the distinct difference between the tracking behavior of the actuator, which, as Fig. 10 shows, is very slow, and the reaction of the actator to disturbance forces. Figure 12 shows the joint angle, held at a constant position, perturbed by pushing on the forearm, then released. When the actuator is released, it swings back to the equilibrium position in about 0.25

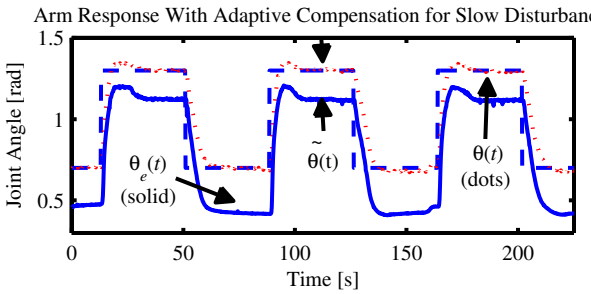

Fig. 11. The arm elbow angle, tracking a desired equilibrium trajectory in the presence of a constant disturbance.

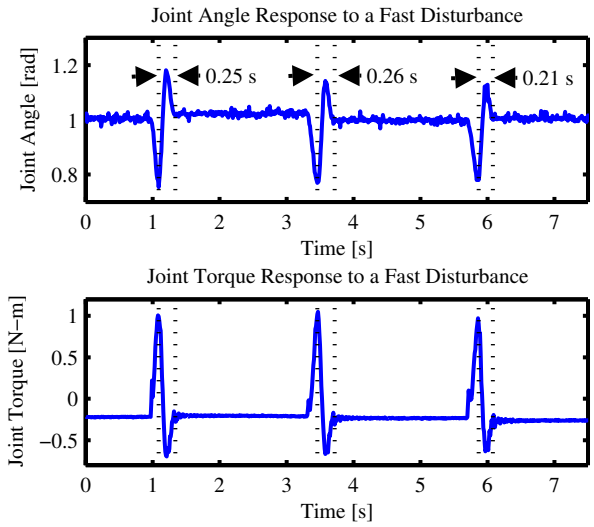

Fig. 12. The response of the actuator to a quick disturbance is much faster than would be expected by the closed-loop system bandwidth.

seconds, much faster than the closed-loop system could possibly react. The reaction torques, also plotted in Fig, 12, indicate that the stiffness of the joint about the desired angle is about 4 Nm/rad. Additionally, the video accompanying this paper shows the actuator tracking a sinusoidal reference in the presence of disturbances (at 0:21), demonstrating that the control system is not at all destabilized by the applied perturbations.

VI. Conclusions

The results presented in this paper are *prima facie* evidence that SMA can be used with closed-loop feedback control to perform human-scale, stable motion control. Instead of trying to scale up an existing control approach effective at the small scale, an architecture more akin to skeletal muscle can be used to decouple the scale of diffusion in the active material from the scale of the force and displacement produced. The scaled-up actuator responds about as quickly as its small motor units do, indicating that the overhead introduced by this recruitment-based control architecture is minimal.

The other take-away lesson from this experiment is that EP control is a useful method for controlling the output force and displacement of a recruitment-based, active material actuator – not because it is a novelty, but because it addresses the structural limitations of the active materials in a constructive fashion, similar to the ways in which it improves the performance of biological actuators. Equilibrium point control provides a way of turning control of the impedance of an actuator into control over more conventional outputs, such as joint angle. It provides a way of responding quickly to disturbance forces that would be otherwise impossible to reject due to activation delays.

VII. Acknowledgments

The authors gratefully acknowledge the assistance of Ian Rust in the fabrication of the experimental apparatus.

This material is based upon work supported by the National Science Foundation under grant number 0143242.

References

[1] Y. Teh and R. Featherstone, "Accurate force control and motion disturbance rejection for shape memory alloy actuators," *2007 IEEE International Conference on Robotics and Automation*, pp. 4454–4459, 2007.

[2] P. Madden, "Development and modeling of conducting polymer actuators and the fabrication of a conducting polymer based feedback loop," Ph.D. dissertation, Massachusetts Institute of Technology, Cambridge, MA, 2003.

[3] A. Mitwalli, "Polymer gel actuators and sensors," Ph.D. dissertation, Massachusetts Institute of Technology, Cambridge, MA, 1998.

[4] E. Henneman, G. Somjen, and D. Carpenter, "Functional significance of cell size in spinal motoneurons," *Neurophysiology*, vol. 28, no. 3, pp. 560–580, May 1965.

[5] L. Odhner, J. Ueda, and H. Asada, "Feedback Control of Stochastic Cellular Actuators," *The 10th International Symposium on Experimental Robotics*, pp. 481–490, 2006.

[6] ——, "Stochastic Optimal Control Laws for Cellular Artificial Muscles," *2007 IEEE International Conference on Robotics and Automation*, pp. 1554–1559, 2007.

[7] J. Ueda, L. Odhner, S.-G. Kim, and H. Asada, "Distributed stochastic control of mems-pzt cellular actuators with broadcast feedback," *Biomedical Robotics and Biomechatronics, 2006. BioRob 2006. The First IEEE/RAS-EMBS International Conference on*, pp. 272–277, 0-0 0.

[8] J. Ueda, L. Odhner, and H. Asada, "Broadcast feedback of stochastic cellular actuators inspired by biological muscle control," *The International Journal of Robotics Research*, vol. 26, no. 11-12, pp. 1251–1265, 2007.

[9] A. Feldman, "Once more on the equilibrium-point hypothesis (λ model) for motor control," *Journal of Motor Behavior*, vol. 18, pp. 17–54, 1986.

[10] J. McIntyre and E. Bizzi, "Servo hypotheses for the biological control of movement," *Journal of Motor Behavior*, vol. 25, no. 3, pp. 193–202, Sep 1993.

[11] F. Lorussi, S. Galatolo, C. Caudai, A. Tognetti, and D. De Rossi, "Compliance control and feldman's muscle model," *Biomedical Robotics and Biomechatronics, 2006. BioRob 2006. The First IEEE/RAS-EMBS International Conference on*, pp. 1194–1199, 2006.

[12] Toki Corporation, "Biometal helix website," August 2009, `http://toki.co.jp/biometal/english/contents.html`.

[13] J. Polit and E. Bizzi, "Characteristics of motor programs underlying arm movements in monkeys," *Journal of Neurophysiology*, vol. 42, no. 1, pp. 183–194, 1979.

[14] J. Park, J. Song, and H. Kim, *Lecture Notes in Control and Information Sciences*. Springer, 2008, vol. 370, ch. Safe Joint Mechanism Based on Passive Compliance for Collision Safety, pp. 49–61.

[15] N. Vitiello, E. Cattin, S. Roccella, F. Giovacchini, F. Vecchi, M. Carrozza, and P. Dario, "The neurarm: towards a platform for joint neuroscience experiments on human motion control theories," *Intelligent Robots and Systems, 2007. IROS 2007. IEEE/RSJ International Conference on*, pp. 1852–1857, 29 2007-Nov. 2 2007.

[16] N. Hogan, "Adaptive control of mechanical impedance by coactivation of antagonist muscles," *Automatic Control, IEEE Transactions on*, vol. 29, no. 8, pp. 681–690, Aug 1984.